Supporting Information

Two-Dimensional Hexagonal Boron Nitride-Ferrofluid Hybrids Enable Efficient Magnetic Cooling

Nishant Tiwari[a, b], Alexey Kartsev[c, d, e], Saswata Goswami[f], Alexander Arkadyevich Safronov[e], Chandra Sekhar Tiwary[a, f], and Varun Chaudhary*[b]*

[a]*Department of Metallurgical and Materials Engineering, Indian Institute of Technology Kharagpur, West Bengal 721302, India*

[b]*Industrial and Materials Science, Chalmers University of Technology, Gothenburg SE-41296, Sweden*

[c]*Bauman Moscow State Technical University, Moscow, Russia, MIREA-Russian Technological University, 119454 Moscow Russia,*

[d]*HSE University, 101000 Moscow, Russia, 101000 Moscow, Russia*

[e]*MIREA-Russian Technological University, 119454 Moscow, Russia*

[f]*School of Nano Science and Technology, Indian Institute of Technology Kharagpur, West Bengal 721302, India*

E-mail: Varunc@chalmers.se

Keywords: magnetic cooling, 2D hBN, ferrofluid, thermal conductivity, DFT

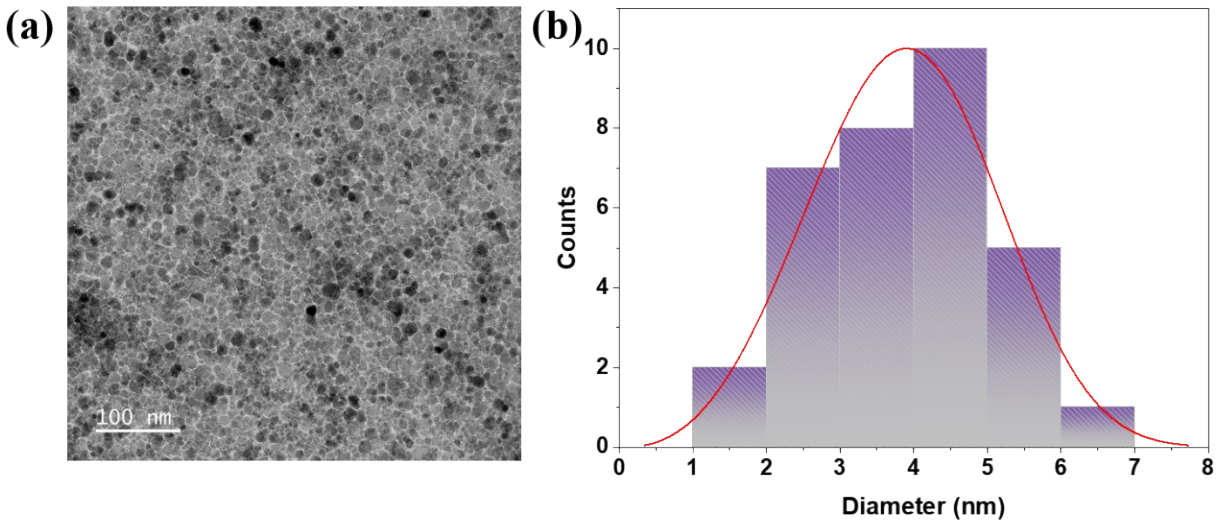

Figure S1 (a) *TEM micrograph of ferrofluid sample* ***(b)*** *Analysed particle size of Mn-Zn-ferrite particles.*

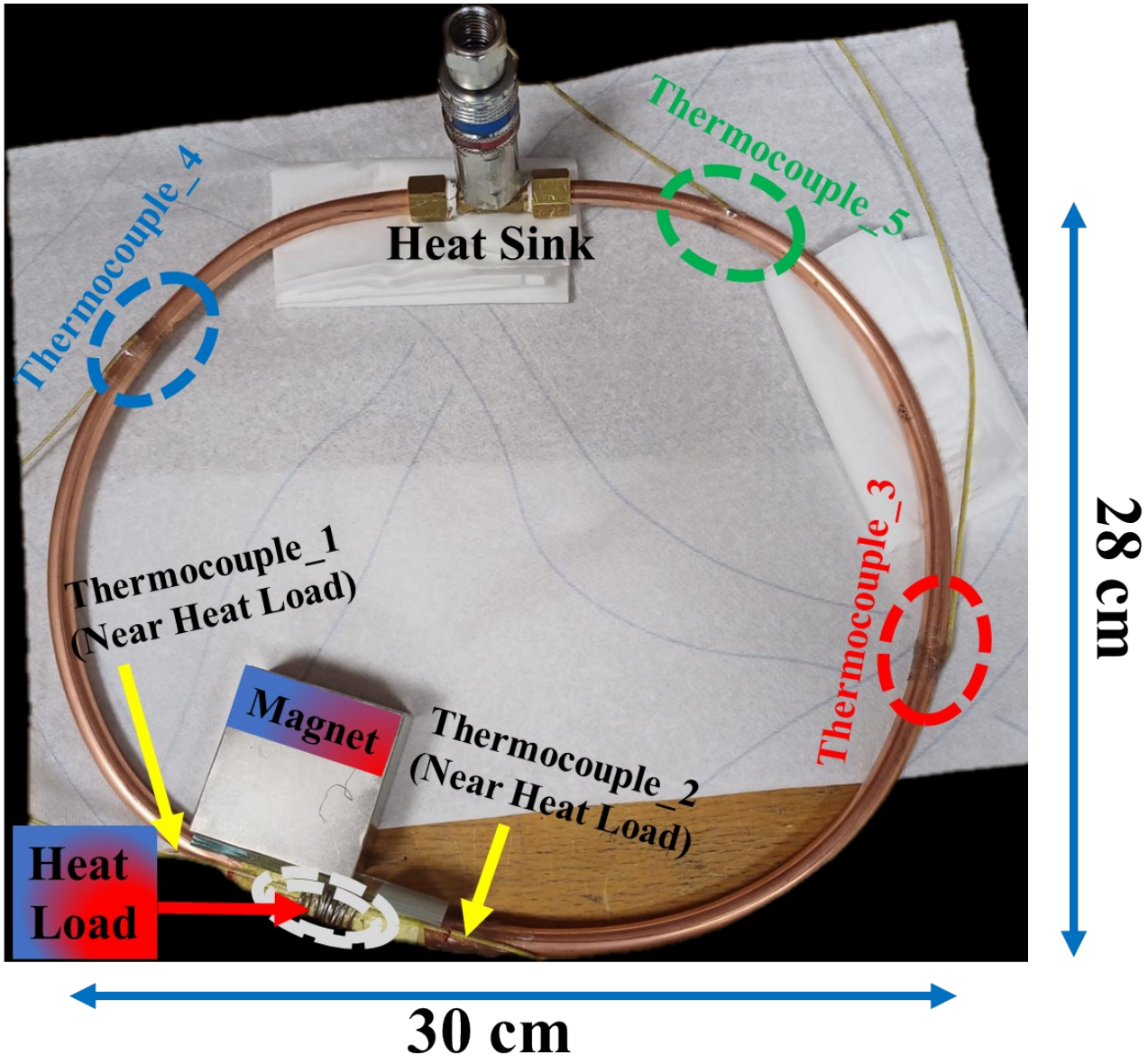

Figure S2 *Copper-based device setup includes a thermocouple, magnet, heat load (Kanthal wire), and heat sink.*

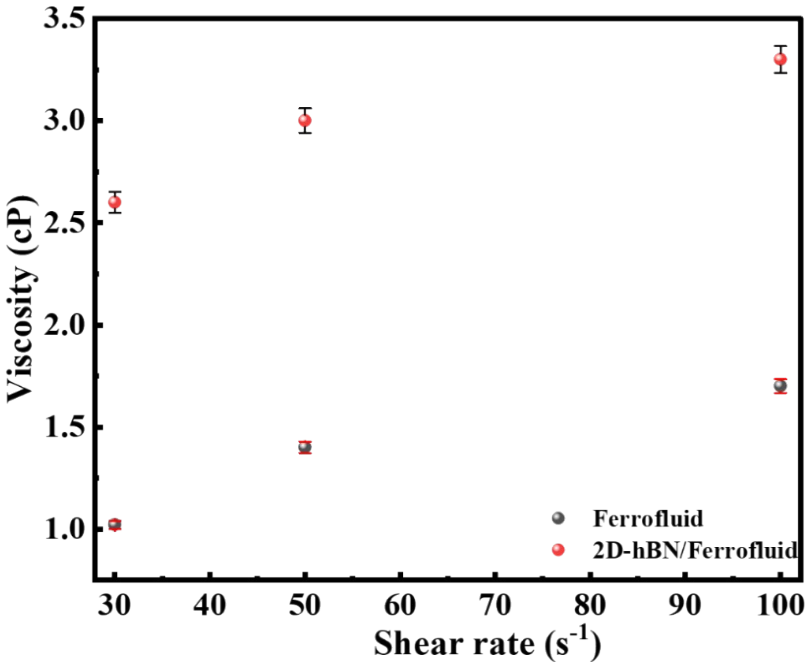

Figure S3 *Viscosity measurement at various shear rates for both the ferrofluid and 2D-hBN/ferrofluid.*

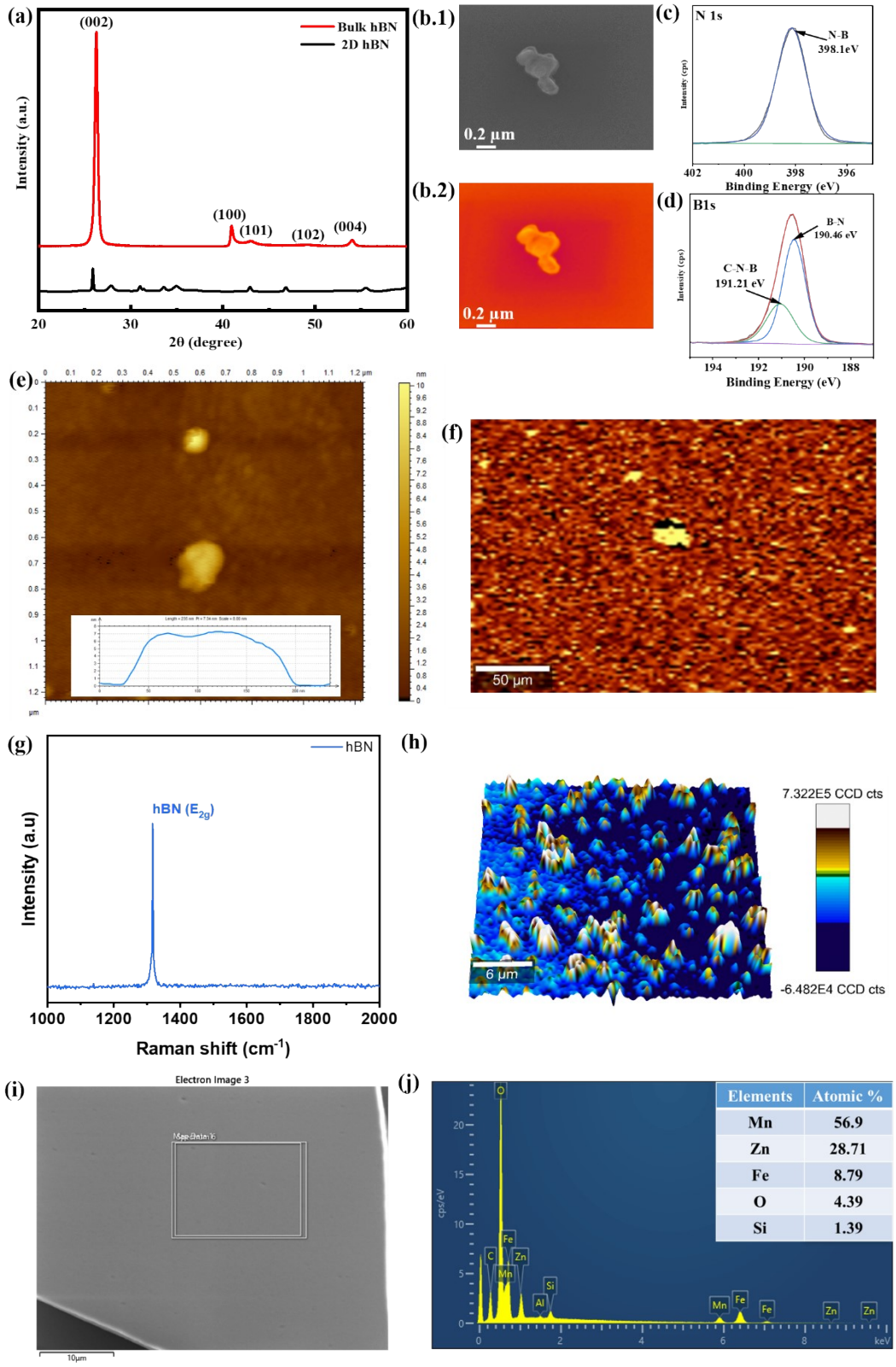

Figure S4 (a) *XRD pattern of bulk hBN (red) and 2D-hBN (black)* ***(b)*** *SEM image of 2D flake of hBN* ***(c, d)*** *XPS analysis of 2D hBN* ***(e)*** *AFM image of 2D-hBN along with the thickness and size of flake* ***(f)*** *Image of Raman Spectra as shown in Fig. 1(b).* ***(g)*** *Raman spectra of 2D-*

hBN ***(h)*** *Image of Raman spectra of 2D-hBN.* ***(i)*** *Secondary electron (SE) image of ferrofluid, which is drop cast on Si-wafer* ***(j)*** *SEM-EDS (Energy dispersive spectroscopy) mapping of SE image.*

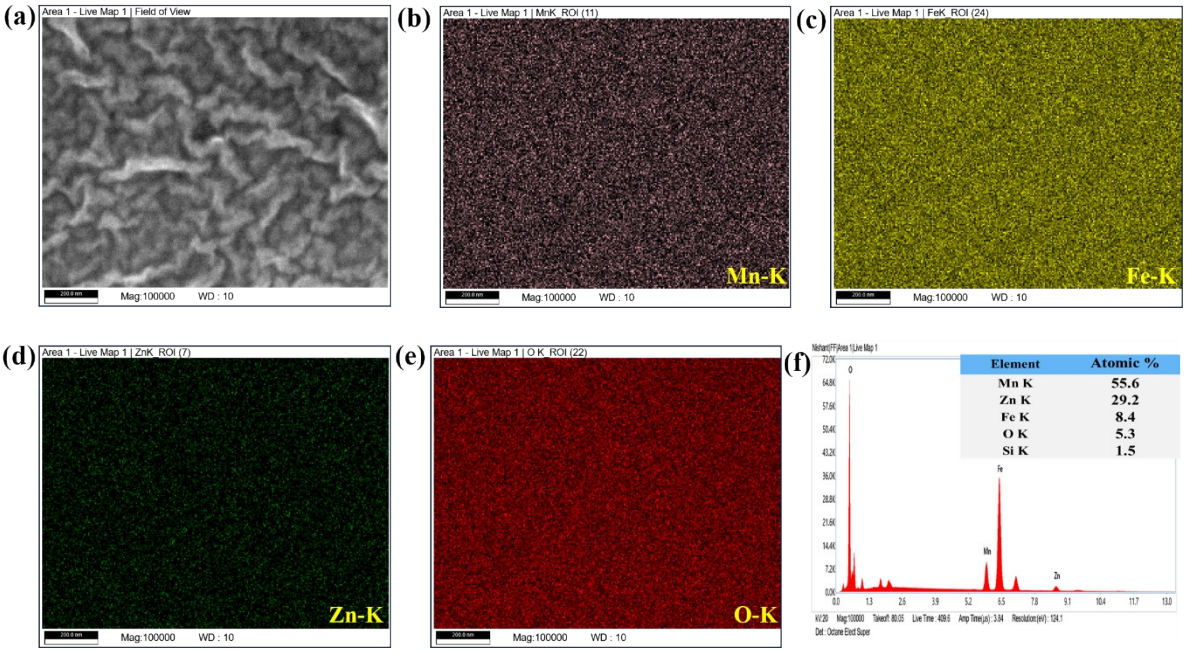

Figure S5 (a) *SEM image of drop casted ferrofluid after sonication* ***(b-e)*** *Elemental distribution of Mn, Fe, Zn and O respectively* ***(f)*** *EDS spectra showing compositional analysis.*

Section S1: Strain measurement

1. TEM based Strain Measurement

To verify the coupling behavior and associated strain transfer mechanism, Geometric phase analysis has been performed on the same microscopic image [1,2]. **Figure S6(a)** depicts the E_{xx}, or the change in the lattice spacing in the x direction. The red region denoting the tensile strain and blue region as compressive strain. **Figure S6(b)** depicts the normal strain in the y direction. The GPA analysis both in xx and yy direction shows the strain induced in x and y direction with nomenclature E_{xx} and E_{yy}. This type of strain gradients induces local polarization and modifies the adsorption energetics. **Figure S6(c)** shows the shear strain E_{xy}, which can indirectly shift the band structure, and can cause flexoelectric response. This type of strain causes the unit cell to become parallelogram. It is defined as

$$E_{xy} = E_{xy} = \frac{1}{2}\left(\frac{\partial u_x}{\partial y} + \frac{\partial u_y}{\partial x}\right)$$

This type strain can detect subtle defect that has been introduced, but has been ignored in the measurement of E_{xx} and E_{yy}. The strain field map delineates the red regions as areas of tensile strain and the blue regions as areas of compressive strain. The alteration in color from blue to red indicated a transition of strain from compression to tension. In the vicinity of an additional half-plane, the strain was compressive and negative owing to the constriction of the normal lattice. The typical lattice was expanding under tensile and positive strain. The maximum E_{xy} strain values were observed at the core region. **Figure S6(d)** shows the lattice rotation compared to reference point. This can be mathematically viewed as,

$$R_{xy} = R_{xy} = \frac{1}{2}\left(\frac{\partial u_y}{\partial x} - \frac{\partial u_x}{\partial y}\right)$$

The sample was put through active sonication period, which might have caused strained lattice on the surface of the material. These high value of R_{xy} can translate to surface level presence of hBN-ferrofluid interface, which is further put in strain through brief sonication period, during heat treatment process. This process identifies the strain behavior while mixing 2D hBN with ferrofluid. The strain has been mainly observed in the junction of the both different type of particles.

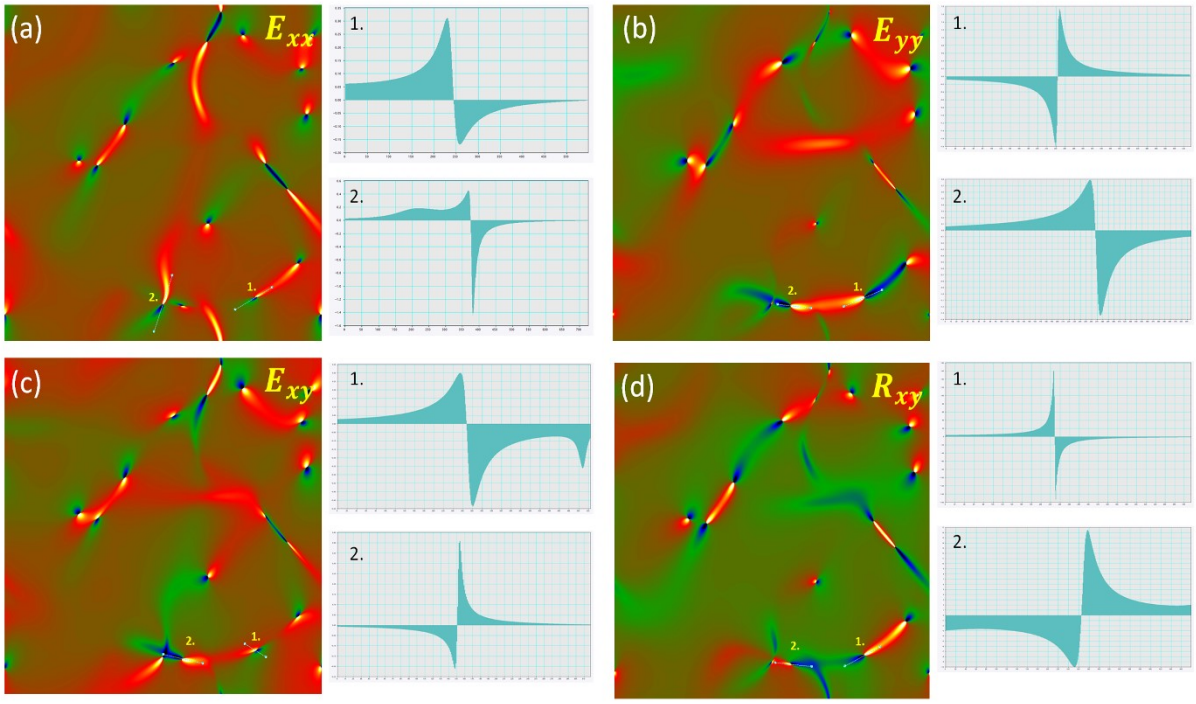

Figure S6 *Figures showing GPA analysis.* ***(a)*** *The strain along the xx direction is denoted as* E_{xx}*. Two lines are drawn to calculate the compressive strain and tensile strain around the 2D -hBN particle suspended in the ferrofluid. These lines are denoted as line 1 and line 2. Positive y value indicates compressive strain, and a negative y value same as that shown for the strain along the* ***(b)*** *yy direction* E_{yy}*,* ***(c)*** *strain along the xy direction* E_{xy}*, and* ***(d)*** *rotational strain* R_{xy}*.*

2. Raman Based Strain Measurement

Figure S7 (a) and (b) show the Raman spectrum-based matching for 2D hBN and Mn-Zn-ferrite ($Mn_{0.7}Zn_{0.3}Fe_2O_4$) nanoparticles, respectively. Raman active material of hBN showing peak around 1366 cm^{-1}. This is E_{2g} mode. Here we have seen point 1 and point 2 window showing 1324 cm^{-1}, while point 3 indicating 1380 cm^{-1} for the E_{2g} mode only. In general, tensile strain translates to Raman peak being shifted to lower wavenumber (Red Shift), and compressive strain translating to Raman peak being shifted to higher wave number (Blue Shift). Point 3 taken at boundary shows tensile stress in 2D hBN structure. This could be due to the shear stress developed during the exfoliation process. The Mn-Zn-ferrite bulk Point 3 to 4 shows shift to lower wavenumber showing red shift, hence compressive strain is shown. The junction shows stress, that has been developed due to mixing or transfer process, creating strained heterostructure of 2D hBN and Mn-Zn-ferrite nanoparticle.

Table S1 Peak value of hBN and Mn-Zn-ferrite nanoparticle at multiple points.

Point window	hBN Peak (cm^{-1})	Mn-Zn-Ferrite (cm^{-1}) [1st peak]	Mn-Zn-Ferrite (cm^{-1}) [2nd Peak]
1	1324	No Peak	No Peak
2	1324	No Peak	No Peak
3	1380	1616	611
4	No Peak	1574	603

As seen in the Table S1, the point window suggests the line along which Raman Spectrum has been taken to deduce the strain behavior amongst the particles.

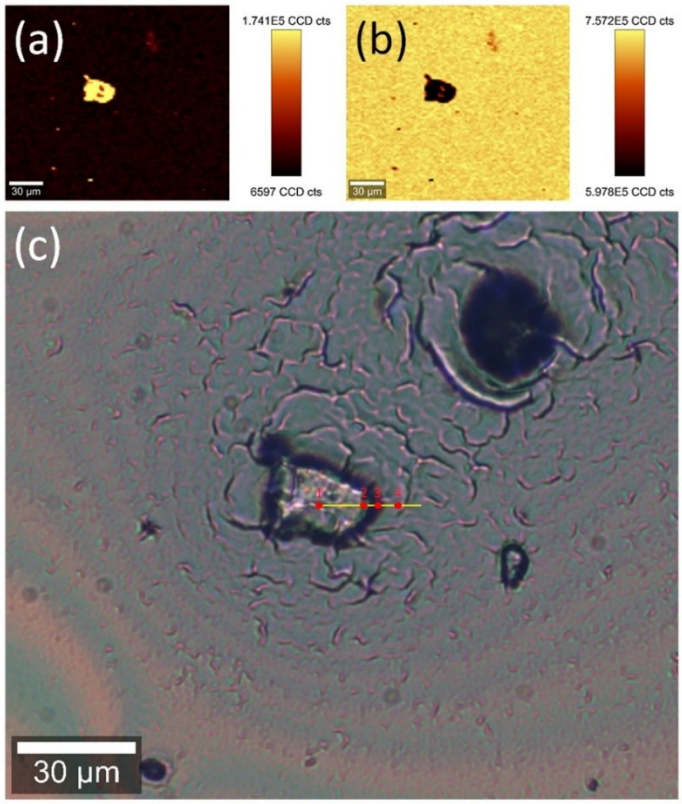

Figure S7 (a-b) *Figures showing Raman Map of 2D hBN and* $MnZnFe_2O_4$ *nanoparticle.* ***(c)*** *Figure showing transferred 2D hBN in Mn-Zn-ferrite nanoparticle matrix. The line depicts along which different points Raman spectrum has been taken.*

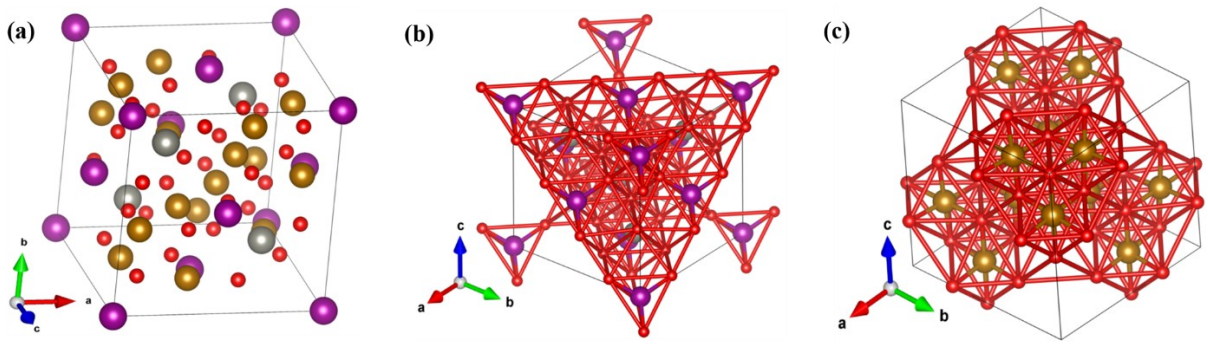

Figure S8. (a) *The elementary cell of $MnZnFe_2O_4$ spinel. Mn ions are shown in purple, Zn ions are shown in gray, Fe ions are shown in yellow, and oxygen ions are shown in red.* ***(b)*** *Mn and Zn ions are shown in the centers of oxygen tetrahedra.* ***(c)*** *Fe ions are shown in the centers of oxygen octahedra.*

Section S2. Comparison with Previous Work

Figure S9 presents the comparison of cooling performance as a function of the applied magnetic field for three systems: the previously reported ferrofluid (black dots)[3], the present ferrofluid (red dots), and the 2D-hBN-based ferrofluid (blue dots). Notably, there are a few differences between the previously reported work and the present study. In earlier work, a polymer tube was used; in this study, a copper (Cu) tube was employed for the device. Additionally, the overall device design also differed between the two studies.

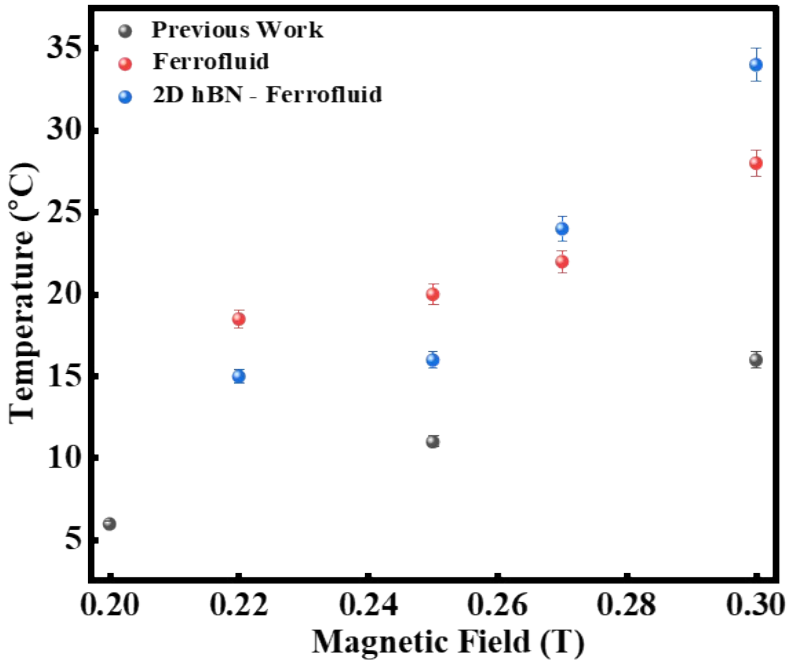

Figure S9. *Comparison of cooling at various magnetic fields with previous work[3].*

A clear enhancement in cooling temperature is observed with increasing magnetic field strength for all samples, demonstrating that higher field intensity facilitates stronger magnetothermal coupling. However, the magnitude of improvement varies significantly among the three systems. The previously reported ferrofluid exhibits a maximum cooling temperature of around 16 °C at 0.30 T, which improves to ~28 °C for the present ferrofluid under identical conditions. Remarkably, the 2D hBN/ferrofluid achieves a substantially higher cooling temperature of nearly 34 °C at 0.30 T, confirming the beneficial role of hBN addition.

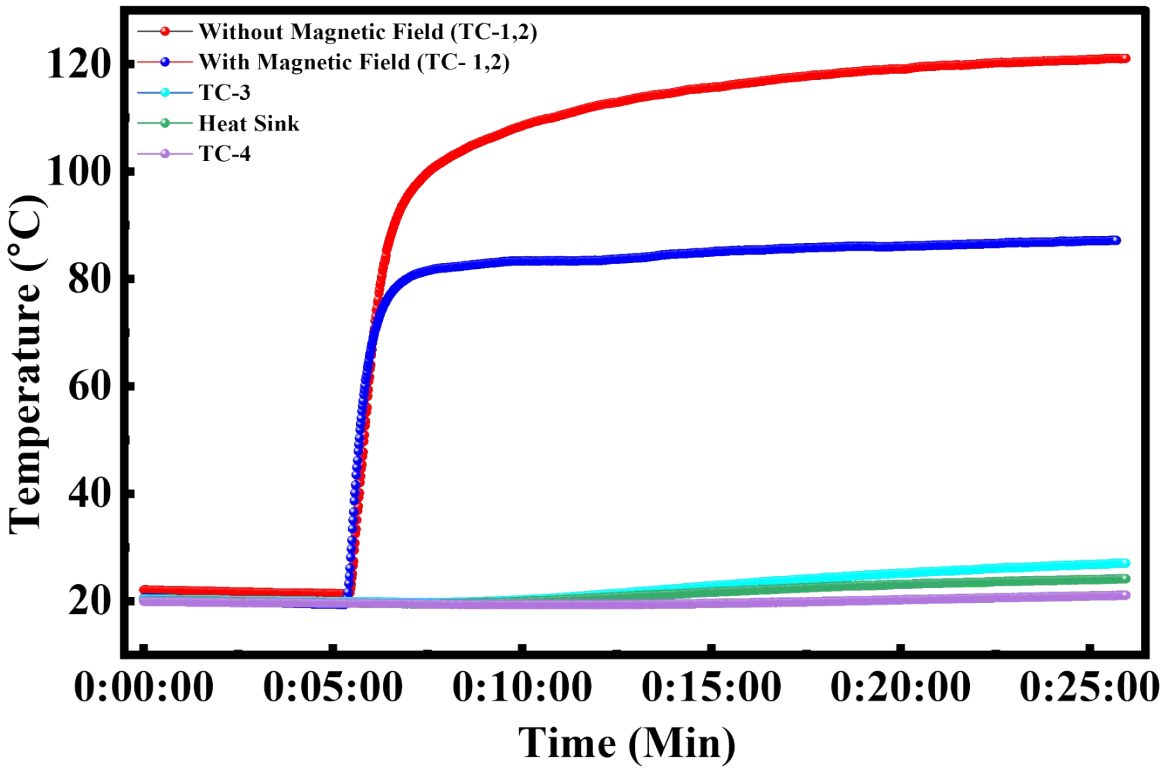

Figure S10 *Effect of magnetic field on 2D hBN/ferrofluid showing the distribution of temperature across the device through TC-1,2, TC-3,4, and TC-5 (Heat Sink).*

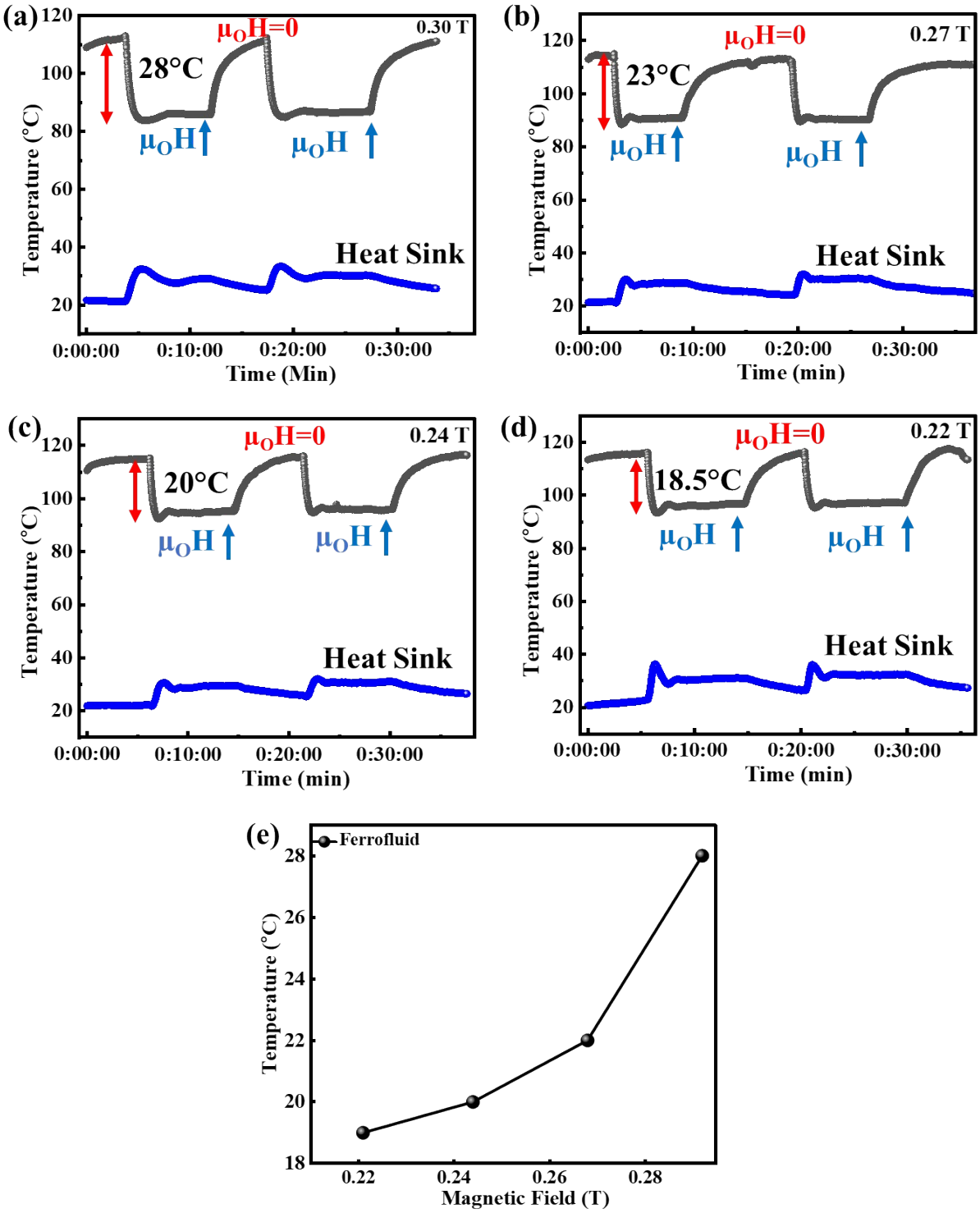

Figure S11. (a-d) *The effect of application and removal of the magnetic field (2 times) for the base ferrofluid and cooling performance of the device at various magnetic fields (0.30 to 0.22 Tesla)* ***(e)*** *Summarized cooling performance in terms of the temperature of the base ferrofluid (black).*

References

1 M. J. H. Hy¨tch, E. Snoeck and R. Kilaas, *Quantitative measurement of displacement and strain fields from HREM micrographs*, 1998, vol. 74.

2 M. Takeda and J. Suzuki, *Crystallographic heterodyne phase detection for highly sensitive lattice-distortion measurements*, 1996, vol. 13.

3 V. Chaudhary, Z. Wang, A. Ray, I. Sridhar and R. V. Ramanujan, *J. Phys. D Appl. Phys.*, DOI:10.1088/1361-6463/aa4f92.